

Terahertz radiation generation by beating of two chirped laser pulses in a warm collisional magnetized plasma

Motahareh Arefnia, Mehdi Sharifian, and Mohammad Ghorbanalilu

Citation: Chin. Phys. B, 2021, 30 (**9**): 094101. DOI: 10.1088/1674-1056/abfb5d
Journal homepage: http://cpb.iphy.ac.cn; http://iopscience.iop.org/cpb

What follows is a list of articles you may be interested in

Direct electron acceleration by chirped laser pulse in a cylindrical plasma channel

Yong-Nan Hu(胡永南), Li-Hong Cheng(成丽红), Zheng-Wei Yao(姚征伟), Xiao-Bo Zhang(张小波), Ai-Xia Zhang(张爱霞), Ju-Kui Xue(薛具奎)
Chin. Phys. B, 2020, 29 (**8**): 084103. DOI: 10.1088/1674-1056/ab943d

Single-order soft x-ray spectra with spectroscopic photon sieve

Yu-Lin Gao(高宇林), Lai Wei(魏来), Qiang-Qiang Zhang(张强强), Zu-Zua Yang(杨祖华), Wei-Min Zhou(周维民), Lei-Feng Cao(曹磊峰)
Chin. Phys. B, 2020, 29 (**5**): 054101. DOI: 10.1088/1674-1056/ab81f0

New hybrid FDTD algorithm for electromagnetic problem analysis

Xin-Bo He(何欣波), Bing Wei(魏兵), Kai-Hang Fan(范凯航), Yi-Wen Li(李益文), Xiao-Long Wei(魏小龙)
Chin. Phys. B, 2019, 28 (**7**): 074102. DOI: 10.1088/1674-1056/28/7/074102

Electron self-injection and acceleration in a hollow plasma channel driven by ultrashort intense laser pulses

Suhui Deng(邓素辉), Mingping Liu(刘明萍)
Chin. Phys. B, 2019, 28 (**4**): 044101. DOI: 10.1088/1674-1056/28/4/044101

Ultra-fast x-ray-dynamic experimental subsystem

Liming Chen(陈黎明), Xin Lu(鲁欣), Dazhang Li(李大章), Yifei Li(李毅飞)
Chin. Phys. B, 2018, 27 (**7**): 074101. DOI: 10.1088/1674-1056/27/7/074101

Terahertz radiation generation by beating of two chirped laser pulses in a warm collisional magnetized plasma

Motahareh Arefnia[1,2], Mehdi Sharifian[2,†], and Mohammad Ghorbanalilu[1]

[1] *Department of Physics, Shahid Beheshti University,* 1983963113, *Tehran, Iran*
[2] *Physics Department, Yazd University, Safaiyeh, Yazd, Iran*

(Received 17 December 2020; revised manuscript received 22 February 2021; accepted manuscript online 26 April 2021)

Analytical equations of terahertz (THz) radiation generation based on beating of two laser beams in a warm collisional magnetized plasma with a ripple density profile are developed. In this regard, the effects of frequency chirp on the field amplitude of the terahertz radiation as well as the temperature and collision parameters are investigated. The ponderomotive force is generated in the frequency chirp of beams. Resonant excitation depends on tuning of the plasma beat frequency, magnetic field frequency, thermal velocity, collisional frequency, and effect of the frequency chirp with the plasma density. For optimum parameters of frequency and temperature the maximum THz amplitude is obtained.

Keywords: plasma, THz radiation, thermal effect, collisional effect, frequency chirp

PACS: 41.75.Jv, 42.25.Bs, 52.25.Xz, 94.20.Fg **DOI:** 10.1088/1674-1056/abfb5d

1. Introduction

In the last three decades, due to the features and potential of the terahertz range, high absorption in water, high transparency in non-conductive materials, and prevention of harmful effects on biological tissues, the terahertz radiation generation have been much attended.[1–5] To produce terahertz radiation energy sources, various methods have been proposed, including the interaction of laser pulses with semiconductors and electro-optic crystals, photoionization of laser pulses composed of both fundamental and second-harmonic waves, laser-plasma interaction, and the other plain.[6–13] As an ionized media plasma has excellent potential for THz generation and there are several schemes in which THz radiation is generated via laser-plasma interaction.[14–20] To increase power and efficiency, in many types of research the external magnetic field is applied to the plasma. The presence of an external magnetic field perpendicular to the direction of laser pulse propagation could increase the radiation efficiency up to several times more than the absence of a magnetic field.[21–26] Since the resonance excitation depends on the tuning of pulse frequency and plasma density, the different types of plasma density, for example, the ripple density, is used to increase the terahertz radiation efficiency.[27–29] The terahertz generation by the beating of two Gaussian laser beams for periodically modulated density in the presence of a static magnetic field has been studied by Malik *et al.*[14] Their analytical calculations show that the resonant excitation of THz under the mentioned conditions is quite effective. They have shown with the optimization of these parameters, the efficiency can be achieved on the order of 10^{-3} or more. On the other hand the effect of temperature and collision frequency in the processes deal with laser–plasma interaction have been studied in several investigations.[30,31] It has been shown that dependency of THz radiation on collision frequency decreases with increasing of the beat wave frequency.[32] Furthermore, THz radiation in the warm collisional plasma by two Gaussian laser beams has been investigated by Niknam *et al.*[33] They have shown that a secondary resonant enhancement appears by considering thermal effects, temperature-dependent collisions at frequency $\omega = \sqrt{\omega_p^2 + k^2 v_{th}^2}$. The effect of frequency chirp has been considered in many cases such as studies on particle acceleration, wakefield generation and terahertz radiation.[34–38] Zhang *et al.*,[34] studied the variation of the chirped 800-nm pulse duration in both experiment and simulation. They revealed that there is the optimum chirp to maximize the THz yield so that extremely sensitive to the temporal propagation. Mehta *et al.*,[39] investigated the sensitivity of the chirping laser on THz generation in a magnetized plasma. It is shown that the duration of nonlinear interaction of laser pulse can increase the frequency chirp.

In the course of this paper, we study THz generation from the chirped lasers beating in a magnetized rippled density plasma by considering collisional frequency and thermal velocity. The static magnetic field applied perpendicular to the direction of the propagation of the beating lasers. The plasma density is periodically changed with wave number α where the periodic plasma density helps to get phase-matching condition and resonant excitation in the THz frequency range. The laser pulses exert the transverse ponderomotive force to the electrons which produces the nonlinear current and finally THz radiation. This paper aims to investigate the effect of frequency chirp on the amplitude of THz radiation in the plasma den-

†Corresponding author. E-mail: mehdi.sharifian@yazd.ac.ir
© 2021 Chinese Physical Society and IOP Publishing Ltd

sity ripple which is affected by thermal effects, temperature-dependent collisions, and external magnetic field.

This paper is organized as follows: in Section 2, the nonlinear current density produced by beating chirped laser pulses is obtained. Then the THz field amplitude is analyzed by calculation of the dielectric permittivity tensor in warm collisional plasma. In Section 3, we examine the numerical results. In Section 4, the conclusion is presented.

2. Theoretical consideration

We consider two Gaussian lasers of same intensity ($I \sim 10^{14}$ W/cm^2), frequency chirp ω_j and wavenumber k_j (where $j = 1,2$) are propagating across (in the x direction) the magnetic field in z direction. The laser beams produce space-periodically density $n = n_0 + n$ where $n = n_\alpha e^{i\alpha x}$, n_0 is uniform plasma density and n_α is amplitude of the ripple. The electric field for laser pulses are given by

$$\boldsymbol{E}_j = \hat{y} E_0 e^{-y^2/a_0^2} e^{i(k_j x - \omega_j t)}, \tag{1}$$

where a_0 is the laser beamwith. Laser pulses are positively chirped as $\omega_1 = \omega_0 + \beta\omega_0^2(t - x/c)$, where ω_0 is initial frequency of the laser in the absence of chirp, β is chirp parameter, and ω_2 is given as $\omega = \omega_1 - \omega_2$, in which ω is frequency of the oscillation. The laser fields impart oscillatory velocities to plasma electrons as

$$\boldsymbol{v}_1 = \frac{e\boldsymbol{E}_1}{m_e\left(i\omega_0 + \beta i\omega_0^2(t - x/c) + \upsilon_e\right)},$$
$$\boldsymbol{v}_2 = \frac{e\boldsymbol{E}_2}{m\left(i\omega_0 + \beta i\omega_0^2(t - x/c) - i\omega + \upsilon_e\right)},$$

where υ_e is the total electron collision frequency including electron–ion and electron–neutral frequencies and written in the form as $\upsilon_e = \upsilon_{en} + \upsilon_{ei}$. The electron ion frequency generally depends on ion density n_i, the degree of the plasma ionization Z_i, the electron temperature T_e, and the Coulomb logarithm $\ln\Lambda$. We choose $\ln\Lambda = 10$, and the electron–ion collision frequency is given as[40]

$$\upsilon_{ei} = \frac{4(2\pi)^{1/2} Z^2 e^2 n_i \ln\Lambda}{3\sqrt{m_e}(K_B T_e)^{3/2}} \approx 2\cdot 9\times 10^{-6}\frac{Z^2 n_i\left(\mathrm{cm}^{-3}\right)\ln\Lambda}{[T_e(\mathrm{eV})]^{3/2}}\ \left[\mathrm{s}^{-1}\right]. \tag{2}$$

Since the neutral density is very low, we neglect the electron–neutral collision (υ_{en}). The ponderomotive potential is defined by $\varphi_p = -(m/2e)\boldsymbol{v}_1\cdot\boldsymbol{v}_2^*$, and the nonlinear ponderomotive force $f_p^{NL} = e\nabla\varphi = -(m/2)\nabla(\boldsymbol{v}_1\cdot\boldsymbol{v}_2^*)$ is modified as follows:

$$f_p^{NL} = -\frac{e^2E_0^2}{2m\left(i\left(\omega_0 + \beta\omega_0^2(t - x/c)\right) + \upsilon_e\right)\left(-i\left(\omega_0 + \beta\omega_0^2(t - x/c) - \omega\right) + \upsilon_e\right)}\left(ik'\hat{x} - \left(\frac{4y}{a_0^2}\right)\hat{y}\right)e^{-2y^2/a_0^2}e^{i(k'x - \omega t)}, \tag{3}$$

where $\omega = \omega_1 - \omega_2$ and $k' = k_1 - k_2$ are beat frequency and wavenumber.

By making use of ponderomotive force the equation of motion in magnetized plasma is written as

$$\frac{\partial\boldsymbol{v}^{NL}}{\partial t} = \frac{e}{m}(\nabla\varphi_p) - (\boldsymbol{v}^{NL}\times\boldsymbol{\omega}_c) - \frac{KT}{mn_0}(\nabla n^{NL}) - \upsilon_e\boldsymbol{v}^{NL}, \tag{4}$$

where $\boldsymbol{\omega}_c = (eB/mc)\hat{z}$ is the cyclotron frequency. The nonlinear electron density obeys the continuity equation $(\partial n^{NL}/\partial t) = -n_0\nabla\cdot\boldsymbol{v}^{NL}$.

By solving Eq. (4) and making use Eq. (3) and nonlinear continuity equation, the nonlinear density perturbation is obtained as

$$n^{NL} = \frac{n_0}{mi\omega\left((i\omega - \upsilon_e)^2 + \frac{KT}{mi\omega}k^2(i\omega - \upsilon_e) + \omega_c^2\right)}\left((i\omega - \upsilon_e)\nabla\cdot\boldsymbol{f}_p^{NL} - \frac{KTk^2}{m\omega}\frac{\partial\boldsymbol{f}_{py}^{NL}}{\partial y} + \nabla\cdot\left(\boldsymbol{f}_p^{NL}\times\boldsymbol{\omega}_c\right)\right). \tag{5}$$

The nonlinear perturbations are affected by ponderomotive force, magnetic field, collisional force, and thermal quiver velocity. Therefore, the space charge field (corresponding potential φ) is generated and then the linear density perturbations is induced, which is given by

$$n^L = \frac{\omega_p^2}{4\pi ei\omega\left((i\omega - \upsilon_e)^2 + \frac{KT}{mi\omega}k^2(i\omega - \upsilon_e) + \omega_c^2\right)}\left((i\omega - \upsilon_e)\nabla\cdot(\nabla\varphi) - \frac{KTk^2}{m\omega}(ik)\left(\frac{\partial\varphi}{\partial y}\right)\right), \tag{6}$$

where $\omega_p = \left(4\pi e^2 n_0/m\right)^{1/2}$ is the plasma frequency. Now by employing the Poisson's equation, $\nabla^2\varphi = 4\pi\tilde{n}e$, where $\tilde{n} = n^L + n^{NL}$ together linear and nonlinear density perturbation, the linear force is obtained as

$$f^L = e\nabla\varphi = \frac{\omega_p^2}{\left(i\omega\left((i\omega - \upsilon_e)^2 + \omega_c^2\right) + \frac{KT}{m}k^2(i\omega - \upsilon_e) - \omega_p^2(i\omega - \upsilon_e)\right)}\left((i\omega - \upsilon_e)\boldsymbol{f}_p^{NL} + i\frac{KTk^2}{m\omega}\boldsymbol{f}_{py}^{NL} + \left(\boldsymbol{f}_p^{NL}\times\boldsymbol{\omega}_c\right)\right). \tag{7}$$

Therefore, the nonlinear velocity components are obtained by using Eq. (4) as

$$v_x^{\mathrm{Nl}} = -\frac{(\mathrm{i}\omega-\upsilon_\mathrm{e})}{(\mathrm{i}\omega-\upsilon_\mathrm{e})^2+\omega_\mathrm{c}^2}\left(\frac{f_{px}^{\mathrm{NL}}}{m}+\frac{f_x^{\mathrm{L}}}{m}\right)-\frac{\omega_\mathrm{c}}{(\mathrm{i}\omega-\upsilon_\mathrm{e})^2+\omega_\mathrm{c}^2}\left[\left(\frac{f_{py}^{\mathrm{NL}}}{m}+\frac{f_y^{\mathrm{L}}}{m}\right)-\frac{KT}{mn_0}\left(\frac{\partial n_y^{\mathrm{NL}}}{\partial y}\right)\right]$$
$$+\frac{(\mathrm{i}\omega-\upsilon_\mathrm{e})}{(\mathrm{i}\omega-\upsilon_\mathrm{e})^2+\omega_\mathrm{c}^2}\frac{KT}{mn_0}\left(\frac{\partial n_x^{\mathrm{NL}}}{\partial x}\right), \tag{8a}$$

$$v_y^{\mathrm{Nl}} = -\frac{(\mathrm{i}\omega-\upsilon_\mathrm{e})}{(\mathrm{i}\omega-\upsilon_\mathrm{e})^2+\omega_\mathrm{c}^2}\left(\frac{f_{py}^{\mathrm{NL}}}{m}+\frac{f_y^{\mathrm{L}}}{m}\right)+\frac{\omega_\mathrm{c}}{(\mathrm{i}\omega-\upsilon_\mathrm{e})^2+\omega_\mathrm{c}^2}\left[\left(\frac{f_{px}^{\mathrm{NL}}}{m}+\frac{f_x^{\mathrm{L}}}{m}\right)-\frac{KT}{mn_0}\left(\frac{\partial n_x^{\mathrm{NL}}}{\partial x}\right)\right]$$
$$+\frac{(\mathrm{i}\omega-\upsilon_\mathrm{e})}{(\mathrm{i}\omega-\upsilon_\mathrm{e})^2+\omega_\mathrm{c}^2}\frac{KT}{mn_0}\left(\frac{\partial n_y^{\mathrm{NL}}}{\partial y}\right). \tag{8b}$$

Now, the nonlinear current density is obtained by $\boldsymbol{J}^{\mathrm{NL}}=-(1/2)n'e\boldsymbol{v}^{\mathrm{NL}}$. It is clear that the nonlinear current is modified by external magnetic field, thermal velocity, nonlinear ponderomotive force, and the linear force due to the self-consistent space-charge field.

The complete form of nonlinear current density components is written in the form as

$$J_x^{\mathrm{NL}} = -\frac{e^3E_0^2n_\alpha}{4m^2\left(\mathrm{i}\left(\omega_0+\beta\omega_0^2(t-x/c)\right)+\upsilon_\mathrm{e}\right)\left(-\mathrm{i}\left(\omega_0+\beta\omega_0^2(t-x/c)-\omega\right)+\upsilon_\mathrm{e}\right)}\frac{(-\mathrm{i}\omega+\upsilon_\mathrm{e})}{\left((-\mathrm{i}\omega+\upsilon_\mathrm{e})^2+\omega_\mathrm{c}^2\right)}\mathrm{e}^{-(2y^2/a_0^2)}$$
$$\times\left[-\mathrm{i}k'+\left(\frac{4y}{a_0^2}\right)-\left(\frac{4y}{a_0^2}\right)\frac{\omega_\mathrm{c}}{(-\mathrm{i}\omega+\upsilon_\mathrm{e})}+\lambda_1\left(\frac{\omega_\mathrm{c}\omega_\mathrm{p}^2}{\left(\mathrm{i}\omega\left((\mathrm{i}\omega-\upsilon_\mathrm{e})^2+\omega_\mathrm{c}^2\right)+\frac{KT}{m}k^2(\mathrm{i}\omega-\upsilon_\mathrm{e})-\omega_\mathrm{p}^2(\mathrm{i}\omega-\upsilon_\mathrm{e})\right)}\right)\right.$$
$$\left.+\lambda_2\left(\frac{\omega_\mathrm{c}\frac{K}{mT}}{\left(\mathrm{i}\omega\left((\mathrm{i}\omega-\upsilon_\mathrm{e})^2+\omega_\mathrm{c}^2\right)+\frac{KT}{m}k^2(\mathrm{i}\omega-\upsilon_\mathrm{e})\right)}\right)\right]\mathrm{e}^{\mathrm{i}(kx-\omega t)}, \tag{9}$$

$$J_y^{\mathrm{NL}} = -\frac{e^3E_0^2n_\alpha}{4m^2\left(\mathrm{i}\left(\omega_0+\beta\omega_0^2(t-x/c)\right)+\upsilon_\mathrm{e}\right)\left(-i\left(\omega_0+\beta\omega_0^2(t-x/c)-\omega\right)+\upsilon_\mathrm{e}\right)}\frac{(-\mathrm{i}\omega+\upsilon_\mathrm{e})}{\left((-\mathrm{i}\omega+\upsilon_\mathrm{e})^2+\omega_\mathrm{c}^2\right)}\mathrm{e}^{-(2y^2/a_0^2)}$$
$$\times\left[\left(\frac{4y}{a_0^2}\right)-\mathrm{i}k'\frac{\omega_\mathrm{c}}{(-\mathrm{i}\omega+\upsilon_\mathrm{e})}+\lambda_3\left(\frac{\omega_\mathrm{c}\omega_\mathrm{p}^2}{\left(\mathrm{i}\omega\left((\mathrm{i}\omega-\upsilon_\mathrm{e})^2+\omega_\mathrm{c}^2\right)+\frac{KT}{m}k^2(\mathrm{i}\omega-\upsilon_\mathrm{e})-\omega_\mathrm{p}^2(\mathrm{i}\omega-\upsilon_\mathrm{e})\right)}\right)\right.$$
$$\left.-\lambda_4\left(\frac{\omega_\mathrm{c}\frac{KT}{m}}{\left(\mathrm{i}\omega\left((\mathrm{i}\omega-\upsilon_\mathrm{e})^2+\omega_\mathrm{c}^2\right)+\frac{KT}{m}k^2(\mathrm{i}\omega-\upsilon_\mathrm{e})\right)}\right)\right]\mathrm{e}^{\mathrm{i}(kx-\omega t)}, \tag{10}$$

where

$$\lambda_1=\left(\frac{8y}{a_0^2}\right)-\frac{KTk'^2}{m\omega(-\mathrm{i}\omega+\upsilon_\mathrm{e})}\left(\frac{4y}{a_0^2}\right)-\mathrm{i}k'\left(\frac{\omega_\mathrm{c}}{(-\mathrm{i}\omega+\upsilon_\mathrm{e})}+\frac{(\mathrm{i}\omega-\upsilon_\mathrm{e})}{\omega_\mathrm{c}}\right),$$
$$\lambda_2=\left(1+\frac{KTk'^2}{m\omega(-\mathrm{i}\omega+\upsilon_\mathrm{e})}\right)\left(\frac{32y}{a_0^4}+\frac{16y}{a_0^4}-\frac{64y^3}{a_0^6}\right)+\mathrm{i}k'\frac{\omega_\mathrm{c}}{(-\mathrm{i}\omega+\upsilon_\mathrm{e})}\left(-\frac{4}{a_0^2}+\frac{16y^2}{a_0^4}\right)+k'^2\left(\frac{4y}{a_0^2}\right)-\mathrm{i}k'^3\frac{(\mathrm{i}\omega-\upsilon_\mathrm{e})}{\omega_\mathrm{c}},$$
$$\lambda_3=2\mathrm{i}k'+\left(\frac{4y}{a_0^2}\right)\left(\frac{\mathrm{i}KTk'^2}{m\omega\omega_\mathrm{c}}-\frac{\omega_\mathrm{c}^2+(\mathrm{i}\omega-\upsilon_\mathrm{e})^2}{\omega_\mathrm{c}(\mathrm{i}\omega-\upsilon_\mathrm{e})}\right),$$
$$\lambda_4=\left(\frac{KTk'^2}{m\omega\omega_\mathrm{c}}-\frac{(\mathrm{i}\omega-\upsilon_\mathrm{e})}{\omega_\mathrm{c}}\right)\left(\frac{32y}{a_0^4}+\frac{16y}{a_0^4}-\frac{64y^3}{a_0^6}\right)+\mathrm{i}k'\left(-\frac{4}{a_0^2}+\frac{16y^2}{a_0^4}\right)-k'^2\left(\frac{4y}{a_0^2}\right)\frac{\omega_\mathrm{c}}{(-\mathrm{i}\omega+\upsilon_\mathrm{e})}-\mathrm{i}k'^3,$$

and $k\equiv k'+\alpha=k_1-k_2+\alpha$ is wavenumber of THz oscillation. We know the nonlinear current responsible for the emission of THz radiation.

The wave equation of THz radiation is obtained by using the Maxwell's equation and can be written as

$$-\nabla^2\boldsymbol{E}+\boldsymbol{\nabla}(\boldsymbol{\nabla}\cdot\boldsymbol{E})=-\frac{4\pi\mathrm{i}\omega}{c^2}\boldsymbol{J}+\frac{\omega^2}{c^2}\bar{\bar{\varepsilon}}\boldsymbol{E}, \tag{11}$$

where, $\bar{\bar{\varepsilon}}$ is the plasma permittivity tensor and given as follow:

$$\bar{\bar{\varepsilon}} = \begin{pmatrix} 1+\dfrac{\omega_p^2}{\left(i\omega(i\omega-\upsilon_e)+\frac{KT}{m}k'^2+\frac{i\omega\omega_c^2}{(i\omega-\upsilon_e)}\right)} & -\dfrac{\omega_p^2\frac{\omega_c}{(i\omega-\upsilon_e)}}{\left(i\omega(i\omega-\upsilon_e)+\frac{KT}{m}k'^2+\frac{i\omega\omega_c^2}{(i\omega-\upsilon_e)}\right)} & 0 \\ \dfrac{\omega_p^2\frac{\omega_c}{(i\omega-\upsilon_e)}}{\left(i\omega(i\omega-\upsilon_e)+\frac{KT}{m}k'^2+\frac{i\omega\omega_c^2}{(i\omega-\upsilon_e)}\right)} & 1-\dfrac{\omega_p^2\left(1+\frac{KT}{mi\omega(i\omega-\upsilon_e)}\right)}{\left(i\omega(i\omega-\upsilon_e)+\frac{KT}{m}k'^2+\frac{i\omega\omega_c^2}{(i\omega-\upsilon_e)}\right)} & 0 \\ 0 & 0 & 1-\dfrac{\omega_p^2}{\omega^2} \end{pmatrix}. \tag{12}$$

By substituting dielectric tensor Eq. (12) in the wave equation of Eq. (11), the wave equation is obtained as

$$\begin{aligned} &\frac{\partial^2 E_{0y}}{\partial x^2}+2ik\frac{\partial E_{0y}}{\partial x}+\left(\frac{\omega^2}{c^2}\left(\frac{\varepsilon_{xy}^2+\varepsilon_{xx}^2}{\varepsilon_{xx}}\right)-k^2\right)E_{0y} \\ &= \lambda_5 E_0\left[\left(\left(\frac{4y}{a_0^2}\right)\left(1+\lambda_8\left(1-\frac{\omega_c}{(-i\omega+\upsilon_e)}\right)\right)-ik'\left(\frac{\omega_c}{(-i\omega+\upsilon_e)}+\lambda_8\right)+\lambda_6(\lambda_3+\lambda_1\lambda_8)-\lambda_7(\lambda_4-\lambda_8\lambda_2)\right)\right]e^{-\left(2y^2/a_0^2\right)}, \end{aligned} \tag{13}$$

where

$$\begin{aligned} \lambda_5 &= \frac{ie\omega\omega_p^2E_0n_\alpha}{4mn_0c^2\left(i\left(\omega_0+\beta\omega_0^2(t-x/c)\right)+\upsilon_e\right)\left(-i\left(\omega_0+\beta\omega_0^2(t-x/c)-\omega\right)+\upsilon_e\right)}\frac{(-i\omega+\upsilon_e)}{\left((-i\omega+\upsilon_e)^2+\omega_c^2\right)}, \\ \lambda_6 &= \frac{\omega_c\omega_p^2}{\left(i\omega(i\omega-\upsilon_e)^2+(KT/m)(i\omega-\upsilon_e)k'^2-\omega_p^2(i\omega-\upsilon_e)\right)}, \\ \lambda_7 &= \frac{\omega_c(KT/m)}{\left(i\omega\left((i\omega-\upsilon_e)^2+\omega_c^2\right)+(KT/m)(i\omega-\upsilon_e)k^2\right)}, \\ \lambda_8 &= -\frac{\omega_p^2\omega_c}{\left(i\omega\left((i\omega-\upsilon_e)^2+\omega_c^2\right)+(KT/m)(i\omega-\upsilon_e)k'^2+\omega_p^2(i\omega-\upsilon_e)\right)}. \end{aligned}$$

Following the phase matching condition in rippled density plasma we use

$$\frac{\omega^2}{c^2}\left(\frac{\varepsilon_{xy}^2+\varepsilon_{xx}^2}{\varepsilon_{xx}}\right)-k^2=0,$$

and obtain the normalized THz radiation field as

$$\left|\frac{E_{0y}}{E_0}\right| = \left|\frac{\lambda_5 x}{2k}\left[\left(\left(\frac{4y}{a_0^2}\right)\left(1+\lambda_8-\lambda_8\frac{\omega_c}{(-i\omega+\upsilon_e)}\right)-ik\left(\frac{\omega_c}{(-i\omega+\upsilon_e)}+\lambda_8\right)+\lambda_6(\lambda_3+\lambda_1\lambda_8)-\lambda_7(\lambda_4-\lambda_8\lambda_2)\right)\right]\right|e^{-\left(2y^2/a_0^2\right)}. \tag{14}$$

3. Results and discussion

In order to examine the effect of frequency chirp, collision frequency, and electron temperature on amplitude of terahertz radiation generated by beat of two chirp laser beams in a magnetized plasma with a ripple density, the numerical analysis of Eq. (14) is investigated. The typical laser and plasma parameters are used to presentation numerical behavior of THz radiation are as follows, $I_L \approx 10^{14}$ W/cm^2, $\omega_0 = 2.4\times10^{15}$ rad/s, $\omega_p = 3\pi\times10^{13}$ rad/s, $t-x/c = 0.5/\omega_p$, $a_0 = 0.08$ cm, $y/a_0 = 0.5$, $n_\alpha = 0.1n_0$, $|v_2^*| = 0.3c$. Figures 1–8 are plotted to show the influence of the thermal effect, temperature-dependent collision frequency, and frequency chirp. Figure 1 shows the variation of THz radiation on the beat frequency for different temperatures. It is seen that THz radiation amplitude decreases rapidly for the higher values of beating frequency. In other words when $\omega\sim\omega_h$, the resonance condition takes place and THz field amplitude reaches its largest value. It can also be seen that normalized THz amplitude is higher at the lower temperatures. Since that, $\omega_h \approx \sqrt{\omega_p^2+\omega_c^2+k^2(KT/m)}$ is upper hybrid frequency, the THz field amplitude acquires a larger value when ω approaches ω_p and for low temperature, $\omega\sim\omega_h$ and close to the resonance condition. To solve the problem more accurately, we analyze the profile of the field amplitude of the THz radiation as a function of temperature for different values of beating frequency in Fig. 2. It seems that THz radiation amplitude increases by increasing the temperature and for a given specific temperature the radiation amplitude is maximum. The opti-

mum temperature for each frequency is different and the optimal value occurs at a higher temperature with the approaching resonance condition. For example, for $\omega/\omega_p = 1.1$ and at $T \approx 0.4$ eV the maximum radiation amplitude is 2×10^{-3}.

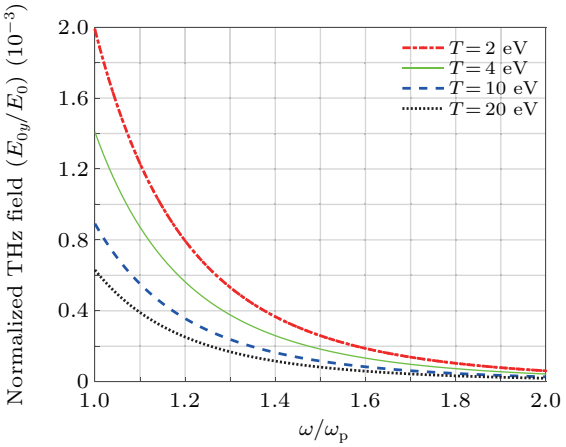


Fig. 1. Normalized amplitude of THz radiation field as a function of normalized beat frequency for different values of temperature when $\omega_c/\omega_p = 0.1$ and $\beta = 2$.

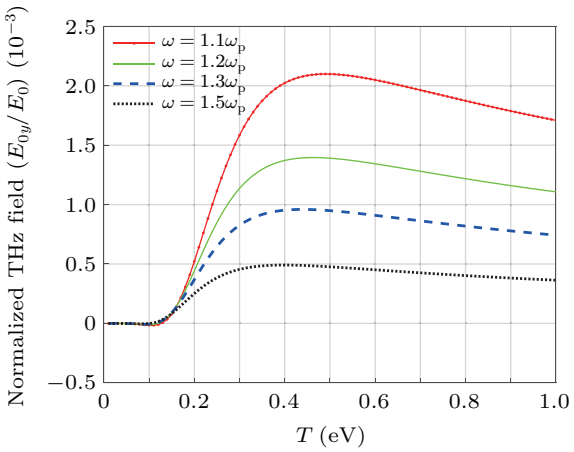


Fig. 2. Normalized amplitude of THz radiation field as a function of temperature for different values of normalized beat frequency. The parameters are the same as those in Fig. 1.

In Fig. 3, we plotted the radiation field amplitude on beat frequency for different values of frequency chirp parameters. We see that for different chirp parameters the maximum amplitude of the THz field accrues still as the beating frequency ω approaches to plasma frequency ω_p, so that the gradient of the curve is sharper for the smaller chirp parameter. The THz field amplitude increases by applying the appropriate chirp parameter where the interaction of beating wave and plasma becomes more effective. The THz field amplitude variation with respect to frequency chirp parameter for different normalized cyclotron frequencies is plotted in Fig. 4. The figure shows that the normalized THz field amplitude increases by decreasing positive chirp and it is more noticeable when the higher magnetic field is applied. The presence of magnetic field helps to tune the frequency and amplitude of the emitted THz. The behaver of curves is in good agreement with three-dimensional (3D) simulation results of Nguyen *et al.*[41]

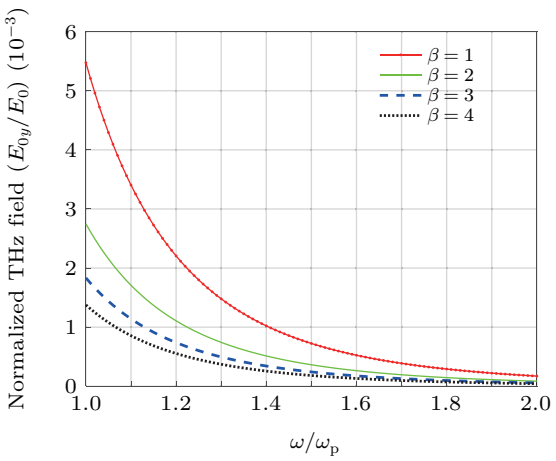


Fig. 3. Variation of normalized amplitude THz radiation field with normalized beat frequency for different values of frequency chirp parameter when $\omega_c/\omega_p = 0.1$, $T = 1$ eV.

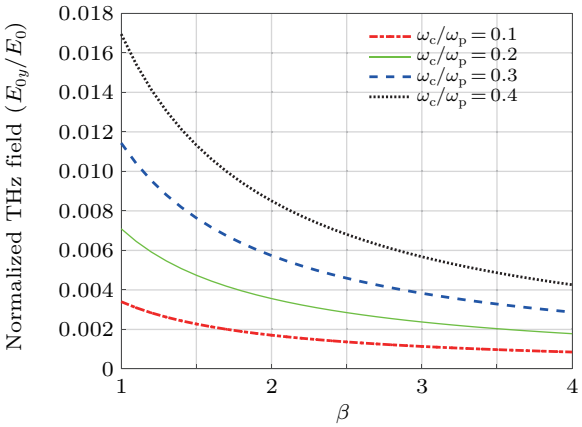


Fig. 4. Variation of normalized amplitude of THz radiation field with frequency chirp parameter for different values of normalized electron cyclotron frequency when $\omega/\omega_p = 1.1$, $T = 1$ eV.

Figure 5 depicted the THz amplitude as a function of β for different values of temperature. It is lucid that the influence of the frequency chirp parameter is dominant for lower temperatures. At the lower temperatures the electron collision frequency is increased and tuned with the frequency chirp.

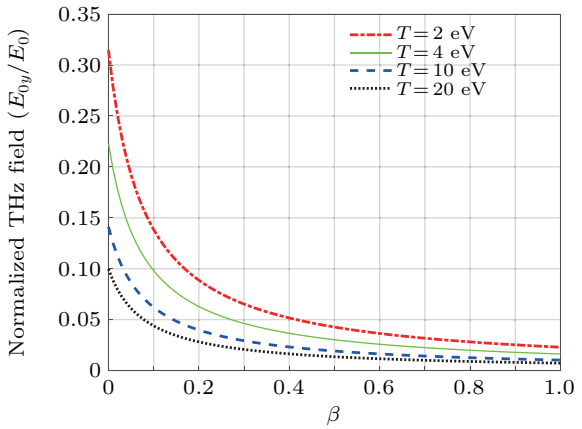


Fig. 5. Normalized amplitude of THz radiation field as a function of frequency chirp parameter for different values of temperature when $\omega_c/\omega_p = 0.1$, $\omega/\omega_p = 1.1$.

In Fig. 6 we analyze the variation of THz amplitude as a function of temperature for different values of negative β.

It is clear that, the THz field attains a peak at a particular value of T. In this region the optimum temperature increases at higher $|\beta|$. Figure 7 shows the dependent of the THz field amplitude on beat frequency and chirp parameter at temperature 0.1 eV. Here, it is observed that a peak appears for the THz field in a value of negative chirp parameter $\beta \approx -0.008$. In Fig. 8 we show the variation of THz amplitude with the temperature and frequency chirp parameter. We find that the THz field amplitude is maximized at the specific negative frequency chirp parameter, so that by increasing the temperature and consequently closer to the resonant excitation the optimum frequency chirp becomes more effective.

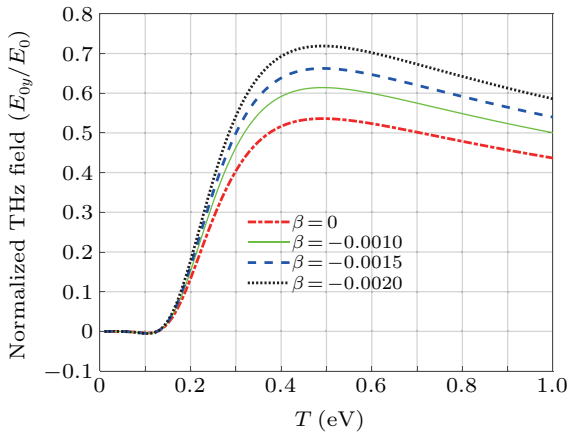


Fig. 6. Normalized amplitude of THz radiation field as a function of temperature for different values of frequency chirp parameter when the parameters are the same as those in Fig. 5.

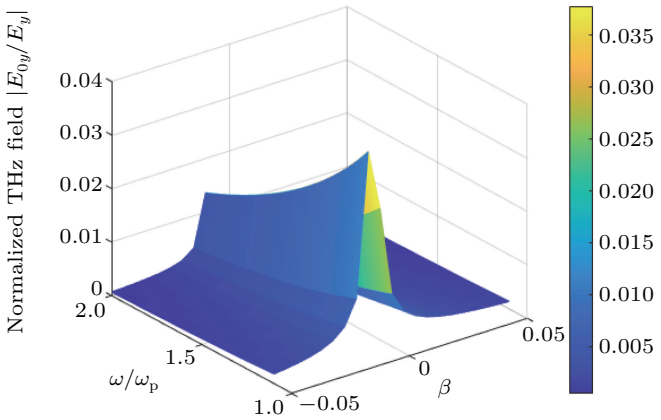


Fig. 7. Spatial normalized amplitude of THz radiation field as a function of normalized beat frequency and frequency chirp parameter for $\omega_c/\omega_p = 0.1$, $T = 0.1$ eV.

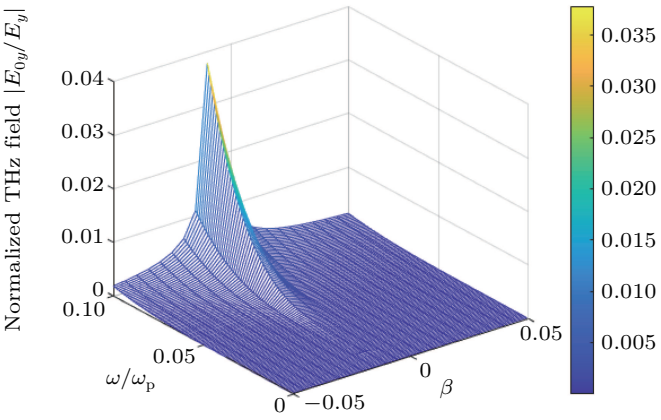


Fig. 8. Spatial normalized amplitude of THz radiation field as a function of temperature and frequency chirp parameter for $\omega/\omega_p = 1.1$, $\omega_c/\omega_p = 0.1$.

4. Conclusion

In this paper, we analytically studied resonant excitation of THz radiation generation by beating two chirped frequency laser beams in the magnetized plasma by considering thermal and collisional effects. In this regard, linear and nonlinear density perturbations and nonlinear current density in frequency chirp are obtained by including thermal velocity and collisional effects in the equation of motion. The amplitude of THz radiation generation by chirped frequency laser is obtained by using the modified permittivity tensor of the plasma and wave equation in the presence of the thermal effect and collision frequency. It was shown that by increasing the magnetic field frequency, temperature (to about 0.4 eV), and consequently decreasing the collision frequency, the resonance excitation is maximized in two frequencies ω_p and $\omega_h = \sqrt{\omega_p^2 + \omega_c^2 + k^2 (KT/m)}$. We know the electron collisional frequency decreases by increasing the temperature, so the electrons move faster and have no chance to collide ions and neutrals. We have shown, that by increasing the positive chirp parameter and consequently decreasing the ponderomotive force and nonlinear current density, the terahertz field amplitude decreases. Also, by increasing of the frequency chirp parameter, the role of temperature becomes less effective. Moreover, we found out a particular region in the negative frequency chirp that the THz amplitude increases with increasing chirp frequency and by approaching to the resonant excitation this increasing becomes more perceptible. This because the frequency chirp allows the electron to remain in the resonance state longer time so that the terahertz amplitude increases as the chirp parameter increases.

References

[1] Mittleman D M 2017 *J. Appl. Phys.* **122** 230901
[2] Chen H, Ma W, Huang Z, Zhang Y, Huang Y and Chen Y 2019 *Adv. Opt. Mater.* **7** 1801318
[3] Tabata H 2015 *IEEE Trans. Terahertz Sci. Technol.* **5** 1146
[4] Van Exter M, Fattinger C and Grischkowsky D 1989 *Opt. Lett.* **14** 1128
[5] Neu J and Schmuttenmaer C A 2018 *J. Appl. Phys.* **124** 231101
[6] Vicario C, Ovchinnikov A, Ashitkov S, Agranat M, Fortov V and Hauri C 2014 *Opt. Lett.* **39** 6632
[7] Ravi K, Huang W R, Carbajo S, Nanni E A, Schimpf D N, Ippen E P and KäRtner F X 2015 *Opt. Express* **23** 5253
[8] Ghaffari-Oskooei S and Aghamir F 2019 *Phys. Plasmas* **26** 033108
[9] Ollmann Z, Fülöp J A, Hebling J and Almási G 2014 *Opt. Commun.* **315** 159
[10] Jepsen P U, Jacobsen R H and Keiding S 1996 *JOSA B* **13** 2424
[11] Singh R K, Singh M, Rajouria S K and Sharma R 2017 *Phys. Plasmas* **24** 103103
[12] Leemans W, Van Tilborg J, Faure J, Geddes C, Tóth C, Schroeder C, Esarey E, Fubiani G and Dugan G 2004 *Phys. Plasmas* **11** 2899

[13] Arkhipov R, Pakhomov A, Arkhipov M, Demircan A, Morgner U, Rosanov N and Babushkin I 2020 *Phys. Rev. A* **101** 043838
[14] Malik A K, Malik H K and Stroth U 2012 *Phys. Rev. E* **85** 016401
[15] Alirezaee H and Sharifian M 2018 *Phys. Plasmas* **25** 043112
[16] Alirezaee H, Sharifian M, Darbani S M R, Majd A E and Saeed M 2020 *IEEE Trans. Plasma Sci.* **48** 576
[17] Alirezaee H, Sharifian M, Darbani S M R, Saeed M, Majd A E and Niknam A R 2020 *Eur. Phys. J. Plus* **135** 342
[18] Bakhtiari F, Esmaeilzadeh M and Ghafary B 2017 *Phys. Plasmas* **24** 073112
[19] Minami Y, Kurihara T, Yamaguchi K, Nakajima M and Suemoto T 2013 *Appl. Phys. Lett.* **102** 151106
[20] Zhao J, Gao H, Li S, Liu C, Chen Y, Peng Y and Zhu Y 2018 *J. Opt.* **20** 105502
[21] Bhasin L and Tripathi V K 2009 *Phys. Plasmas* **16** 103105
[22] Sedaghat M, Ettehadi-Abari M, Shokri B and Ghorbanalilu M 2015 *Phys. Plasmas* **22** 033114
[23] Yoshii J, Lai C, Katsouleas T, Joshi C and Mori W 1997 *Phys. Rev. Lett.* **79** 4194
[24] Malik A K, Singh K P and Sajal V 2014 *Phys. Plasmas* **21** 073104
[25] Kumar M, Bhasin L and Tripathi V 2010 *Phys. Scr.* **81** 045504
[26] Bogatskaya A, Gnezdovskaia N and Popov A 2020 *Phys. Rev. E* **102** 043202
[27] Kumar S, Singh R K, Singh M and Sharma R 2015 *Laser Particle Beams* **33** 257
[28] Kumar M, Tripathi V K and Jeong Y U 2015 *Phys. Plasmas* **22** 063106
[29] Thakur V, Kant N and Vij S 2020 *Phys. Scr.* **95** 045602
[30] Zhang X B, Qiao X, Cheng L H, Tang R A, Zhang A X and Xue J K 2015 *Phys. Plasmas* **22** 094502
[31] Ettehadi-Abari M, Sedaghat M, Shokri B and Ghorbanalilu M 2015 *Plasma Phys. Control. Fusion* **57** 085001
[32] Sharifian M, Sharifinejad H and Golbakhsi H 2014 *J. Plasma Phys.* **80** 453
[33] Niknam A, Banjafar M, Jahangiri F, Barzegar S and Massudi R 2016 *Phys. Plasmas* **23** 053110
[34] Zhang Z, Panov N, Andreeva V, Zhang Z, Slepkov A, Shipilo D, Thomson M, Wang T J, Babushkin I and Demircan A 2018 *Appl. Phys. Lett.* **113** 241103
[35] Rezaei-Pandari M, Jahangiri F and Niknam A R 2019 *Laser and Particle Beams* **37** 242
[36] Rezaei-Pandari M, Niknam A, Massudi R, Jahangiri F, Hassaninejad H and Khorashadizadeh S 2017 *Phys. Plasmas* **24** 023112
[37] Razavinia S and Ghorbanalilu M 2019 *Phys. Rev. Accelerators and Beams* **22** 111305
[38] Razavinia S and Ghorbanalilu M 2020 *Plasma Phys. Control. Fusion* **62** 045007
[39] Mehta A, Rajput J and Kant N 2019 *Laser Phys.* **29** 095405
[40] Eliezer S 2002 *The interaction of high-power lasers with plasmas* (CRC Press)
[41] Nguyen A, de Alaiza Martínez P G, Thiele I, Skupin S and Bergé L 2018 *New J. Phys.* **20** 033026